

# TEMPERATURE EFFECTS ON GEOTECHNICAL PROPERTIES AND SOLUTE TRANSPORT PROCESSES IN CLAY

Ei Ei MON<sup>1)</sup>, Shoichiro HAMAMOTO<sup>1)</sup>, Toshiko KOMATSU<sup>1)</sup>, and Ken KAWAMOTO<sup>1)</sup>  
<sup>1)</sup> Soil Mechanics Lab., Department of Civil and Environmental Engineering, Saitama University

## ABSTRACT

Recently, the utility of ground source heat pumps (GSHP) systems in public area is increasingly being popular in all over the world but it is leading to the concerns of possible temperature effects on geotechnical properties of sediments as well as solute transport processes in geoenvironment. In this study, temperature effects on geotechnical properties of kaolin clay (consolidation characteristics, shear stiffness, and permeability), solute transport processes in kaolin clay (KCl diffusion) and (KCl sorption) were investigated under three temperatures ranging from 5 °C to 40 °C by modified oedometer tests, by specified volume diffusion tests, and by batch adsorption tests, respectively. The higher in temperature resulted in the greater in geotechnical properties such as apparent preconsolidation pressure ( $P_{ac}$ ) and shear stiffness ( $G_{b,e}$ ) whereas saturated hydraulic conductivity ( $K_{sat}$ ) increased with increasing temperature. On the other hand, the high temperature significantly enhanced the mobility of both ions in the clay with the increase in solute diffusivity ( $D_s/D_0$ ) approximately as one sixth of water saturated porosity in linearly. Accordingly, this study revealed that solute/contaminants transport in porous media rather than geotechnical properties of clay sediments should be concerned as a critical issue under elevated temperature condition.

**KEYWORDS:** temperature, consolidation, shear stiffness, solute diffusion, and sorption

## 1. INTRODUCTION

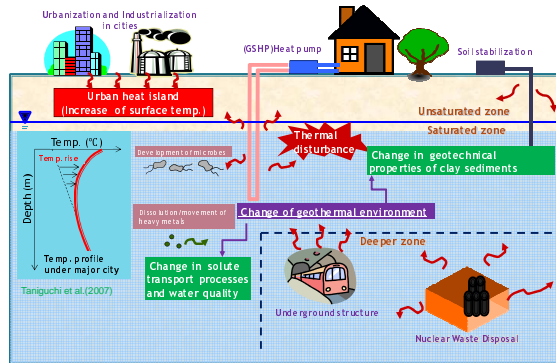


Figure 1 Existence of thermal disturbances in and its consequential effects on geoenvironment.

In a few decades, large underground facilities such as underground railways, expressways, ground source heat pump (GSHP) systems and nuclear waste repositories have been widely constructed in both shallow and deeper zones of earth with various purposes. On the other hand, thermal (heat) disturbances discharged from the facilities and systems consequently likely induce subsurface temperature anomalies since the local temperature anomalies (cold or heat plumes) have been documented in some studies (Haehnlein *et al.*,

2010; Bonte *et al.*, 2011, Sower *et al.*, 2006). Hence, it should be paid a great deal of attention as an important global issue because it may alter soil-water systems associated with geotechnical properties of clay sediments, solute/mass transport processes, groundwater quality, and microbial activities in porous medium (Fig. 1). Comprehending temperature effects on the above mentioned properties and processes in soil-water systems is crucial to address the issues related to subsurface temperature variations.

Recently, GSHP systems have become increasingly popular and been used in public areas (schools, hospitals) with the purpose of acquiring energy for heating and cooling with minimal climate impact such as green house gas emission (Spitler *et al.*, 2005; Omer, 2008). The GSHP system exchanges heat by extracting heat for indoor heating (winter situation) and by rejecting heat for cooling (summer situation) (Florides and Kalogirou, 2007). Temperature variation up to around  $\pm 10^{\circ}\text{C}$  in subsurface monitoring wells in the near vicinity of GSHP systems has been observed in several countries (Sowers *et al.*, 2006; Bonte *et al.*, 2011). At present, the unified knowledge of temperature effects on geotechnical properties and solute diffusion processes particularly considering

for the elevated and depressed local subsurface temperature is still required to perform risk assessments of geoenvironmental impacts by such GSHP systems. Consequently, temperature variation caused by the seasonal operation of GSHP systems, therefore, was targeted in this study by considering local typical ground temperature of 15°C in Kanto area, Japan (Taniguchi *et al.*, 2007) as a reference temperature of  $\pm 10^\circ\text{C}$  variation. Furthermore, a temperature of 40°C was selected as an extreme, representing a temperature change of 25 °C and better allowing comparison with previous studies.

A review of previous studies in the previous section pointed out that temperature is one of the major factors which govern the geotechnical properties and solute transport processes in clays. Although several studies of temperature related issues have been available, present study was conducted in order to fulfill the lack of information and measurements observed in previous studies. Thus, temperature effects on geotechnical properties and solute transport process in clay in particular as a function of void ratio ( $e$ ) or water-saturated porosity of the clay (related to soil pore structure) were investigated in this study.

The general objectives of this study are (1) to examine temperature effects on geotechnical (consolidation, shear stiffness, and permeability) properties of kaolin clay using modified oedometer tests in terms of the parameters such as apparent preconsolidation pressure ( $P_{ac}$ ), shear stiffness ( $G$ ), and permeability ( $k$ ) as a function of void ratio, (2) to investigate temperature effects on solute transport processes (solute diffusion using specified volume diffusion tests (SVD) and sorption using batch sorption tests) in kaolin clay in terms of the parameters such as solute diffusion coefficient ( $D_s$ ) as a function of void ratio, and adsorption coefficient ( $K_f$ ).

## 2. MATERIALS AND METHODS

### 2.1 Materials

In this study, kaolin clay (non-swelling clay) was selected as a model material prior to the use of natural sediments collected from 50 m depth bore holes which were used as monitored wells around a heat exchange tube of a GSHP system in Saitama University Campus, Japan. The information from this study would represent for properties and processes in fine grained soils (cohesive soils). The liquid limit (69%) and plasticity index (39%) of the clay were measured under room temperature (20 °C). The  $N_2$  specific surface area (representing the external surface area of particles) and the particle density were also measured, yielding 16.25  $\text{m}^2/\text{g}$  and 2.658  $\text{g}/\text{cm}^3$ . The preconsolidated kaolin samples with different void ratios were used in both modified oedometer tests and SVD tests. Firstly, the kaolin slurry was made by mixing the

kaolin powder and distilled water at 200% water content. Air bubbles were removed from the slurry by vacuuming for one hour. Then, the slurry was poured into the column. The slurry was loaded under different pressures up to the maximum applied consolidation pressure ( $P_c$ ) of 150 kPa for modified oedometer tests and 220 kPa for SVD tests. For modified oedometer tests, high  $e_0$  and low  $e_0$  were attained by varying standard duration of loads.

The potassium chloride (KCl), one of the most abundant chemical compounds in soil-water system, was selected as a tracer solution for solute transport process in clay. It is existent in soil-water system through various pathways such as rock weathering process or application of K fertilizers. In SVD tests, 0.1 M KCl solution having approximately about 4000 ppm of  $\text{K}^+$  and 3550 ppm of  $\text{Cl}^-$  was used as a tracer solution for diffusion process. In batch equilibrium sorption tests, a wide range of five different initial concentrations of  $\text{K}^+$  (100, 500, 1000, 2000, and 4000 ppm) was used to have a comparison with the concentration used in SVD tests.

### 2.2 Methods

#### 2.2.1 Modified oedometer tests

The laboratory experiments for the measurements of geotechnical properties of the clay were conducted by a modified oedometer apparatus as shown in Fig. 2.

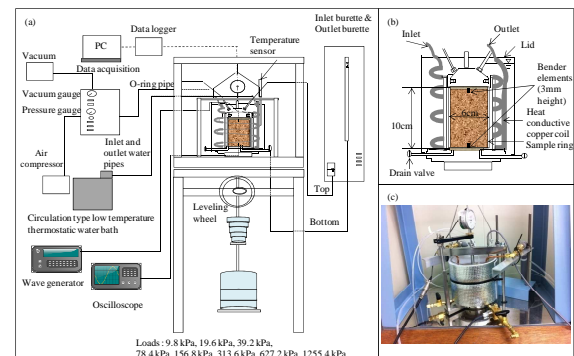


Figure 2 (a) Overview of a modified oedometer apparatus (b) detail of sample cell (c) photo of sample cell.

The standard oedometer apparatus was modified by installing heat conductive copper coils, bender elements, and inlet and outlet burettes to measure consolidation settlement and shear wave velocity simultaneously, as well as hydraulic conductivity. The specified temperature can be maintained throughout the consolidation test by circulating cool non-freezing liquid or hot water from the circulation type low temperature thermostatic water bath (Thomas, TRL-11LP) to the heat conductive copper coils (Habibagahi, 1973; Viridi and Keedwell, 1988). The sample ring inside the water-filled cell was heated indirectly by

the surrounding water (heated by the spirally placed copper coils). Water temperature inside the cell was measured by a temperature sensor which provides the feedback signal to the circulation bath. The bender element system has been recently developed for the measurement of soil stiffness at very small strains in the laboratory by means of elastic shear wave propagation (Lee and Santamarina, 2005; Chan, 2010). In the new apparatus (Fig. 2), the 3-mm long bender elements were placed at opposite ends of the kaolin specimen by installing a pair of bender elements in top cap and base of the cell. The travel time between a transmitter (bender element at top cap) and a receiver (bender element at the base) was determined using a wave generator (nF, Wavefactory WF 1943A 1CH), and a digital storage oscilloscope (Hitachi, VC-6723A). Since a measurement of hydraulic conductivity by the falling head method was carried out immediately after the consolidation test at each applied pressure, the O-ring was inflated by an air compressor, and the drain valve was closed to seal the system thereby avoiding the continued consolidation process. Then, distilled water was applied from the bottom (from the inlet burette) to the top (to the outlet burette) of the kaolin sample while the hydraulic conductivity measurement was conducted. Water level in the inlet burette was observed as a function of time. After the hydraulic conductivity test, the O-ring was deflated by a vacuum and the consolidation test was continued by loading at a higher pressure.

Sequential measurements of consolidation settlement, shear wave velocity, and hydraulic conductivity were performed under the given temperature conditions (5°C ~ 40°C). Additionally, consolidation settlement and shear wave velocity were simultaneously measured under temperature elevation condition from 15°C to 40°C in the secondary compression stage of two particular applied consolidation pressures. After each test, the undisturbed samples (0.7 cm x 0.7 cm) were collected and freeze-dried in the freeze-dry chamber. The pore size distribution of tested sample was measured by Mercury Intrusion Porosimeter (MIP). Shear modulus ( $G_{b,e}$ ) was calculated by

$$G_{b,e} = \rho \times (v_s)^2 \quad (1)$$

where  $\rho$  is the density of the sample (g/cm<sup>3</sup>), and  $v_s$  is the shear wave velocity (m/sec).

### 2.2.2 Specified volume diffusion tests (SVD)

Each diffusion test was performed adopting a two-chamber system so called a specific volume diffusion (SVD) apparatus to obtain diffusion coefficients for preconsolidated or compacted kaolin clay as shown in Fig. 3. The SVD apparatus

was developed by Rowe *et al.* (2000) particularly intended for expansive material like bentonite where the height (or volume) of the sample is specified. Thus, it allows the greater control of total porosity of the specimen during the test. The whole set up was made from of acrylic material except steel rods which fasten the rings. It consists of two plates (top and bottom), and three rings (upper, middle, and lower) where the middle ring looks like sandwich with the sealing of two acrylic plates (H 0.3 mm) on both sides of the ring.

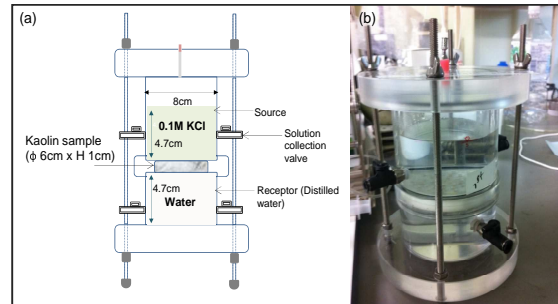


Figure 3 (a) Schematic diagram and (b) photo of a specified volume diffusion apparatus.

The kaolin sample ( $\phi$  6 cm x H 1 cm) was collected from the preconsolidated column using a cutting shoe. Then, it was put into the middle ring and the apparatus was fixed up as shown in Fig. 3. It was saturated with distilled water from bottom to up. After saturation process, the distilled water in the upper ring was removed. Then, it was filled with 0.1 M KCl solution up to 4.71 cm to have a similar volume of distilled water in the lower ring. Diffusion was generally driven from the source to receptor by concentration gradient between two chambers. About 3 ml of solution from the source and the receptor were collected at different time intervals (i.e. 1, 3, 5, 7, 10, 15, 20, 30, 45, 60 days). Then, the removed fluid was replaced by an equivalent amount of distilled water. Then, the collected sample solution was diluted 20 times and 10 times with distilled water for sample from the source and the receptor, respectively. The diluted solutions were filtered and measured pH and EC of the solutions. The ion concentrations in the diluted solutions were analyzed by Ion Chromatography (IC). After termination of each SVD test, pore size distribution measurements were performed by MIP.

### 2.2.3 Batch adsorption tests

The standard batch method recommended in the Organization for Economic Co-operation and Development (OECD, 2000) was used to determine KCl adsorption with the highest adsorption efficiency. Prior to equilibrium sorption isotherm experiments, kinetics experiments for sorption were required. Batch kinetic experiments were performed by collecting triplicate samples at each different time (i.e., 10 min, 30 min, 45 min, 1 hr, 2

hr, and 3 hr) for two initial concentrations of potassium ( $K^+$ ) (500 ppm and 2000 ppm) at two different temperatures (6 °C and 40 °C). Equilibrium sorption isotherm experiments were carried out at five high concentrations of  $K^+$  (100, 500, 1000, 2000, and 4000 ppm) in triplicate at three temperatures (6 °C, 15 °C, 40 °C) under equilibrium condition. All samples were prepared in 50 mL NALGENE™ centrifuge tubes by mixing kaolin clay (2.5 g) and KCl solution prepared in Milli-Q water (10 mL) in 1:4 (w/w) ratios (Manassero *et al.*, 1996). All samples were kept on the temperature control shaker for shaking 24 hours in equilibrium tests and shaking above mention different times in kinetics tests at 200 rpm under each temperature condition. The centrifuge tubes were then put in the high speed refrigerated centrifuge (TOMY, SRX-201) at 12000 rpm for 10 minutes. After centrifugation, 7 mL of the supernatant out of 10 mL of sample solution from each tube was decanted for kinetics or equilibrium concentration analysis. The removed supernatant was then filtered through 0.22  $\mu$ m filters for kaolinite. The equilibrium pH values of the filtered solutions were measured by pH meter (HORIBA, AS-211). The equilibrium concentrations of potassium ( $K^+$ ) and chloride (Cl) in the filtered solutions ( $C_e$ ) were also analyzed by Ion Chromatography. The difference between the initial and equilibrium concentrations was assumed to be due to adsorption.

### 3. RESULTS AND DISCUSSION

#### 3.1 Temperature effects on geotechnical properties (Part 1): Simultaneous measurements of consolidation characteristics, shear stiffness, and permeability under sequential consolidation pressures at different temperatures

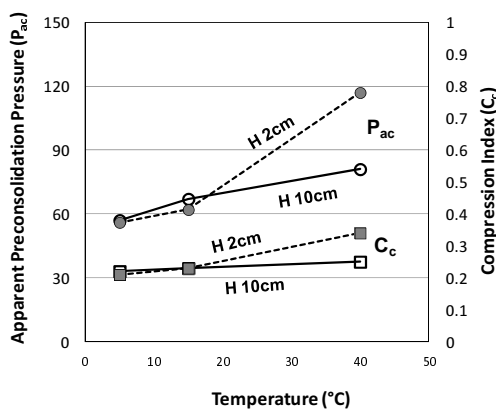


Figure 4 Effect of temperature on apparent preconsolidation pressure ( $P_{ac}$ ) and compression index ( $C_c$ ) for H 2 cm and H 10 cm samples with high  $e_0$  ( $1.5 < e_0 < 1.65$ ).

Previously, some researchers reported a decrease in apparent preconsolidation pressure

( $P_{ac}$ ) at higher temperature for natural undisturbed clays and remolded clays (Tidfors and Sallfors, 1989; Boudali *et al.*, 1994; Campanella and Mitchell, 1968). A clear and opposite trend for samples with high void ratio was observed in this study as shown in Fig. 4. Apparent preconsolidation pressure ( $P_{ac}$ ) and compression index ( $C_c$ ) increased with temperature significantly for H 2 cm samples. Crawford (1964) suggested that the influence of temperature on the preconsolidation pressure is strongly dependent on the testing technique. Thus, the discrepancies may be caused by different sample properties such as initial void ratio and clay fabric structure due to differences in pretreatment method, heating or cooling periods, applied preconsolidation pressure ( $P_c$ ), and different experimental procedures or testing techniques. In summary, the consolidation parameters ( $P_{ac}$ ,  $C_c$ , etc.) which reflect the consolidation characteristics of the kaolin clay were dependent on temperature under most conditions.

Under both 5 °C and 40 °C conditions, the shear modulus increased sharply with decreasing void ratio (increasing consolidation pressure) in overconsolidated state while it increased gradually in normally consolidated state. Thus, the shear stiffness property of the kaolin clay with respect to applied consolidation pressure was found to be stress state dependent. Interestingly, a larger shear modulus at higher temperature was found with 30% to 10% increment between 5°C and 40°C conditions, even at the same void ratio (Fig. 5).

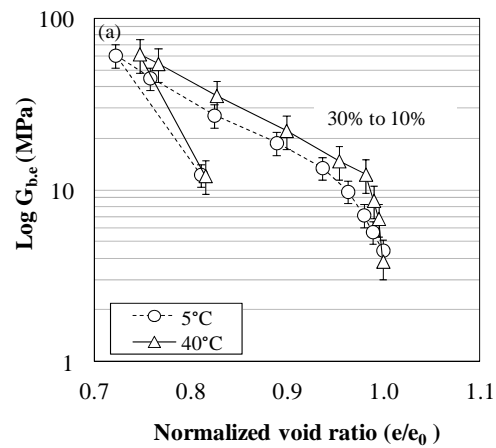


Figure 5 The relationships between shear modulus ( $G_{b,e}$ ) and normalized void ratio ( $e/e_0$ ) for H 10 cm samples with high  $e_0$ , obtained after 24 hours of each pressure (stress) step, at 5 °C and 40 °C.

Typically, sample strength properties such as stiffness represent the soil state and structure. Thus, the present result indicates that fabric structure of kaolin clay, which is determined by the arrangements and subsequent adjustments in inter-particle forces between clay particles (Nakagawa *et*

al., 1995), was possibly influenced by temperature. Lambe (1960) described that the electrical attractive forces at particle level in clays strongly govern the engineering behavior of soils. The inter-particle forces between clay particles such as Coulombic forces and van der Waals forces vary inversely with the dielectric constant property of the pore medium which is temperature dependent property (Sridharan and Rao 1979; Rao and Sridharan 1985). The dielectric constant of water,  $k$ , decreases with increasing temperature, for instance the dielectric constant at 40 °C is 15% less than at 5 °C. As a result, the strong inter-particle forces between particles at 40 °C might enhance microscopic physico-chemical interactions between particles in assemblage, causing that the shear stiffness of kaolin clay increased with temperature. Hence, the increase of shear stiffness at 40 °C may correspond to increase in apparent preconsolidation pressure ( $P_{ac}$ ) at 40 °C, suggesting highly interrelated mechanical properties under the consolidation process. However, since marked temperature effects on consolidation characteristics were only observed for samples with higher initial void ratio, the assumed heat induced changes in inter-particle forces may be significant only for high porous materials.

The relationship between permeability and void ratio was described by the Kozeny-Carman equation (Scheidegger, 1957),

$$k = \frac{n^3}{5A_m^2(1-n)^2} \quad (2)$$

where  $k$  is intrinsic permeability ( $\text{cm}^2$ ),  $A_m$  is specific surface (volume based specific surface area) ( $\text{cm}^{-1}$ ), and  $n$  is porosity, related to void ratio by  $n = \frac{e}{1+e}$ .

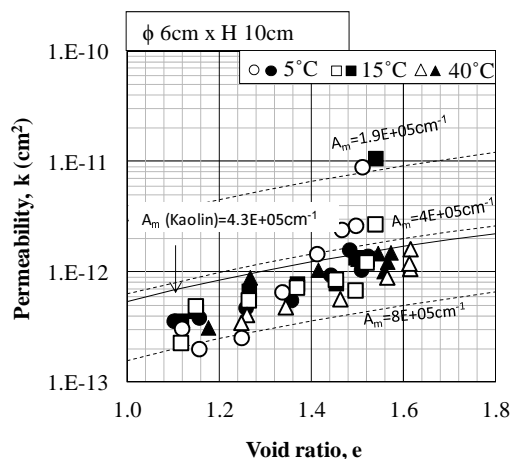


Figure 6 The correlations between water permeability ( $k$ ) and void ratio ( $e$ ). The dotted lines are the predicted lines with respect to specific surface area ( $A_m$ ) using the modified Kozeny-Carman equation. The solid line shows the predicted line using the measured specific surface

area of kaolin clay. Open symbols represent the data obtained from direct measurement and filled symbols represent the data obtained by the modified oedometer using Terzaghi's theory of one-dimensional consolidation.

In Fig. 6, the permeability of the kaolin clay is shown as a function of void ratio with increasing applied consolidation pressure. The measurements for H 10 cm samples were done by both direct measurement in the modified oedometer and Terzaghi's theory. Predictive model lines using the Kozeny-Carman equation (Eq. 2) (with  $A_m$  set equal to  $N_2$  measured volume specific surface area) were added in Fig. 6 in order to confirm the likely permeability range of the tested kaolin clay. For both H 10 cm samples, permeability values ranged from  $10^{-13} \text{ cm}^2$  to  $10^{-11} \text{ cm}^2$ , and agreement with the Kozeny-Carman equation was relatively good for both direct and theory measurements. This implies a good performance of the modified oedometer apparatus for measuring water permeability. For both H 10 cm and H 2 cm samples sizes, the coefficient of intrinsic permeability ( $\text{cm}^2$ ) generally decreased with decreased void ratio. The reason for this permeability behavior as a function of void ratio is that particle assemblages become closer with increasing consolidation pressure (decreasing void ratio), and the subsequent reduction in total void space causes a reduction in water permeability. The measurements indicated that permeability of kaolin clay for both samples was less affected by temperature. But, the hydraulic conductivity was basically influenced by temperature due to temperature dependent pore water properties (viscosity and density). Similar observations were reported by Abuel-Naga *et al.* (2006) on the hydraulic properties for soft Bangkok clay, showing temperature dependent hydraulic conductivity property whereas intrinsic permeability showed no temperature dependency up to 100 °C.

However, the measurements of permeability and pore-size distribution of samples revealed that temperature effects on macroscopic pore structure governing water permeability are less significant within the studied temperature range (5 °C to 40 °C).

### 3.2 Temperature effects on geotechnical properties (Part 2): Change in consolidation settlement and shear modulus induced by temperature elevation in the secondary compression stage under two consolidation pressures

Temperature elevation in secondary compression stage was performed at two consolidation pressures which represent overconsolidated (OC) state and normally consolidated (NC) state for samples with high  $e_0$  ( $1.5 < e_0 < 1.65$ ) and low  $e_0$  ( $1.4 < e_0 < 1.5$ ).

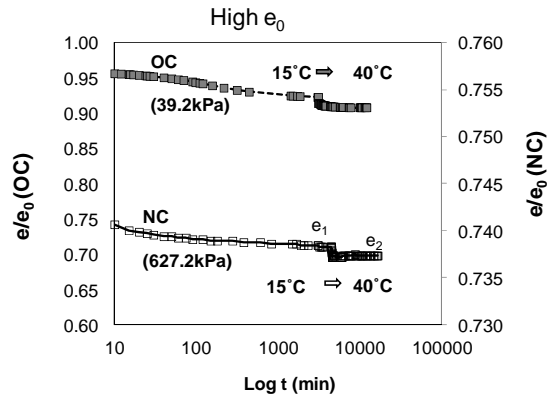


Figure 7 Variation of normalized  $e$  with time for samples with high  $e_0$  at 39.2 kPa (OC clay) and 627.2 kPa (NC clay). Note: 1440 minutes equal to 1 day.

In general, when the samples were consolidated, high void ratio of both OC samples and NC samples decreased with time in both primary consolidation and secondary compression stages at a constant temperature of 15 °C. It was basically due to dissipation of pore water in primary consolidation stage and the strengthening of physico-chemical bonds between particles in secondary compression stage (Anderson and Stokoe, 1978; Nakagawa *et al.*, 1995). The controlled temperature was raised to 40 °C after two days when there was no settlement caused by the applied stress/pressure in the secondary compression stage. The void ratio of the sample was gradually dropped after temperature change for both samples indicating that heating reactivated the consolidation settlement in secondary compression stage (Towhata *et al.*, 1993; Shimizu, 2003). It seemed that the lower pore water viscosity at high temperature accelerated the deterioration of the structure of clay particles under a substantial stress. The similar results were also reported in Towhata *et al.* (1993).

There was a sudden dropped down variation as soon as after temperature elevation to 40 °C for both OC and NC samples as seen in Fig. 8. Then, larger shear modulus,  $G_{b,e}$  ( $G_2$ ) was obtained after being heated for 7 days at 40 °C for OC samples whereas the shear modulus did not recover after the drop for NC samples. This may likely resulted from either temperature influence on the performance of bender element measurement or the adjustment of clay particles during temperature change which probably induce the higher stiffness at high temperature (40 °C). Previously, the effect of temperature on shear strength properties have been found to be strongly dependent on the volume changes induced by heating so called thermal consolidation (Sultan *et al.*, 2000). Accordingly, the increase in consolidation settlement after temperature elevation might reflect the greater shear stiffness at 40 °C particularly for OC samples.

The soil stiffness is generally determined from contact interactions, particle packing arrangement, and elastic stiffness of the solids. Thus, the enhanced inter-particle forces between clay particles at 40 °C by smaller dielectric constant property of pore water might result in the greater shear stiffness at 40 °C since the clays with high  $e_0$  under OC state possessed greater pore water volume. This verified the hypothesis of increase in  $G_{b,e}$  at high temperature mainly resulted from temperature dependent possible fabric structure as described in previous section (part 1).

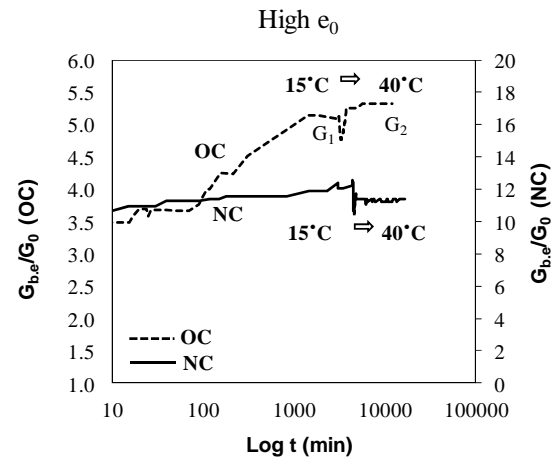


Figure 8 Variation of normalized  $G_{b,e}$  with time for samples with high  $e_0$  at 39.2 kPa (OC clay) and 627.2 kPa (NC clay). Note: 1440 minutes equal to 1 day.

### 3.3 Temperature effects on solute transport processes (Part 1): Solute diffusion in preconsolidated kaolin clay at different temperatures

Temperature effects on solute transport (diffusion) process were highly significant showing larger solute diffusion coefficients ( $D_s$  or  $D_{s, app}$ ) at 40 °C for both  $Cl^-$  and  $K^+$  ions mainly due to less water viscosity at higher temperature. Diffusion of  $K^+$  was delayed (retarded) compared to that of  $Cl^-$  mainly due to  $K^+$  adsorption on clay particles. The solute diffusion coefficients ( $D_s$  or  $D_s$ ) were evaluated by two chamber method (Semi Analytical Solution). The only five sampling data (5 days, 7 days, 10 days, 15 days, 20 days) were used for linearization of the regression line for deducing of precise  $D_s$  in diffusion process

The obtained solute diffusion coefficients of both ions for samples at two different bulk densities under three temperature conditions (Fig. 9). The solute diffusion coefficient for both ions increased with increasing temperature mainly due to the lower viscosity of water at higher temperature as well as due to the faster activated ion motion at higher temperature. The similar trend was observed as in previous studies such as the diffusion of a group of volatile aromatic

hydrocarbons of a geosynthetic clay liner (GCL) at two temperature (7 °C and 22 °C) (Rowe *et al.*, 2005), and diffusion of Zn and Cd through natural clay within temperature range between 15 °C and 55 °C (Do and Lee, 2006). The positive correlations between  $D_{s, app}$  and temperature provided the higher coefficient of determination ( $R^2 > 0.95$ ). The results indicated that  $D_s$  increased by around  $(0.031 \text{ to } 0.036) \times 10^{-10} \text{ m}^2\text{s}^{-1}$  times temperature for  $\text{Cl}^-$  and  $(0.027 \text{ to } 0.033) \times 10^{-10} \text{ m}^2\text{s}^{-1}$  times temperature for  $\text{K}^+$ . The  $\text{Cl}^-$  ion has relatively higher diffusion coefficient than  $\text{K}^+$  ion with the ratio of  $D_s(\text{Cl}^-)/D_{s, app}(\text{K}^+)$  ranging only from 1.1 to 1.2 probably due to the slight retardation of  $\text{K}^+$  by sorption of clay particles. The independent batch adsorption experiments were carried out in next section to verify this observation. As a result, solute diffusion was highly influenced by temperature not only for heavy metal diffusion in swelling clays but also for other dissolved chemical diffusion in non-expansive clays through temperature dependence of pore water property.

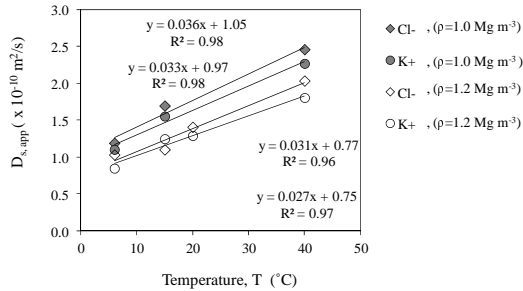


Figure 9 Apparent solute diffusion coefficients ( $D_{s, app}$ ) for both ions as a function of temperature.

For the literature data of solute diffusivity, eight soils included sandy, silty, and clayey soils were used and data represent diffusion coefficient of conservative, inorganic solutes in porous media with relative water saturation ( $\theta/\phi$ ) larger than 0.9 and a total porosity ( $\phi$ ) larger than  $0.1 \text{ cm}^3\text{cm}^{-3}$ . The measured  $D_s/D_0$  under different temperatures and literature  $D_s/D_0$  are plotted against water-saturated porosity ( $\phi$  or  $\theta_{sat}$ ). For the literature data of gas diffusivity, the data sets were used for the  $D_p$  at air saturation of sand, natural soils, clay minerals and Bentonite. The literature  $D_p/D_0$  data are plotted against air filled porosity (Fig. 10). The linear Penman model which assumes a linear variation of gas diffusivity with air-filled porosity ( $\epsilon$ ) using a constant tortuosity factor (0.66) is generally adapted to describe the solute diffusivity (Penman, 1940). The Penman model is given as,

$$\frac{D_s}{D_0} = 0.66\phi \text{ or } \frac{D_s}{D_0} = 0.66\theta_{sat} \quad (3)$$

where  $D_s$  is solute diffusion coefficient ( $\text{m}^2/\text{s}$ ),  $D_0$  is self-diffusion coefficient in free water ( $\text{m}^2/\text{s}$ ) which

can be calculated for respective temperature and respective ion. As seen in Fig. 10a, Penman model was quite applicable to predict solute diffusion coefficient only for the soils. However, the measured data for solute diffusion ( $\text{Cl}^-$ ,  $\text{K}^+$ ) in kaolin clay was mostly predicted by using the following relationship,

$$\frac{D_s}{D_0} = 0.166\phi \text{ or } \frac{D_s}{D_0} = 0.166\theta_{sat} \quad (4)$$

This illustrated that both  $\text{Cl}^-$  and  $\text{K}^+$  ions has higher solute diffusivity at higher void ratio with  $D_s/D_0 \sim 1/6 \phi$  (water-saturated porosity). It was 4 times lower than solute diffusivity in soils probably due to the smaller/finer pore system in kaolin clay which reduced the solute diffusion efficiency. In addition, it would probably be  $D_s/D_0 \sim 1/12 \phi$  for pure clay mineral bentonite possibly indicating more tortuous path ways in liquid phase for solute diffusion in such mineral having inter particle layers.

As early as the beginning of the last century, Buckingham (1904) suggested a simple, one-parameter power law model originally for gas diffusivity; hence, it is also used for solute diffusivity:

$$\frac{D_s}{D_0} = \theta_{sat}^X \quad (5)$$

where  $\theta_{sat}$  is the volumetric water content at saturation ( $\text{m}^3\text{m}^{-3}$ ), and  $X$  is an exponent characterizing pore connectivity - tortuosity. This means that solute diffusivity increased with increasing volumetric water content. Buckingham (1904) proposed  $X=2$  while Marshall (1959) and Millington and Quirk (1959) reported  $X=1.5$  and 1.33, respectively. Then, these three existing models as a function of total porosity (or saturated volumetric water content) were drawn in Fig. 10b. The Millington and Quirk (1959) and Marshall (1959) models were fitted well for gas diffusivity in sands while Buckingham (1904) model was fitted well for both solute and gas diffusivity in natural soils. The fitting curves provided around  $X \sim 4.4$  for kaolin clay in the present study,  $X \sim 8$  for clay minerals from Currie (1960) and Kozaki *et al* (2001) and  $X \sim 10$  for bentonite from the literature. This indicated that the exponent characterizing pore connectivity - tortuosity is greater for clay minerals especially bentonite than natural soils. Both ions showed higher solute diffusivities at higher void ratio corresponding to lower bulk density: with  $D_s/D_0 \sim 1/6\theta_{sat}$  (water-saturated porosity) using linear model and with  $D_s/D_0 \sim (\theta_{sat})^{4.4}$  using non-linear power model.

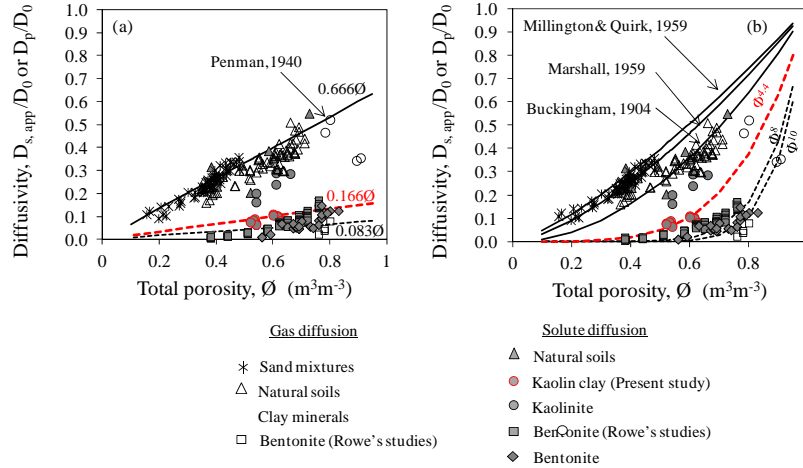


Figure 10 Diffusivity of solute diffusion ( $D_{s,app}/D_0$ ) or gas diffusivity ( $D_p/D_0$ ) as a function of water-saturated total porosity ( $\emptyset$ ) which is equal to saturated volumetric water content ( $\theta_{sat}$ ) for measured data as a comparison with literature data (a) linear model (b) nonlinear model.

### 3.4 Temperature effects on solute transport processes (Part 2): Sorption of KCl on kaolin clay at different temperatures

The effects of temperature on KCl sorption on kaolin clay were examined for both  $K^+$  and  $Cl^-$ . However, almost no chloride adsorption was observed since it is a conservative ion. Thus, the adsorption of potassium onto kaolin clay was discussed through equilibrium sorption isotherms, kinetic adsorption behaviors, and thermodynamic adsorption behaviors.

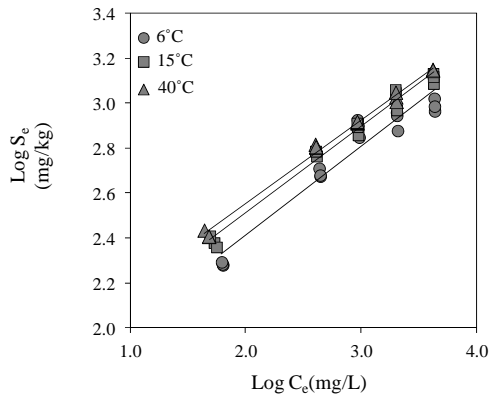


Figure 11 Freundlich isotherm plot for  $K^+$  sorption onto kaolin clay at three different temperatures.

The linear Freundlich model can be expressed as

$$\log S_e = \log K_f + \frac{1}{n} \log C_e \quad (6)$$

when  $S_e$  is the adsorbed amount of adsorption in equilibrium (mg/kg),  $C_e$  is the final concentration of potassium or chloride (mg/L),  $K_f$  is the Freundlich adsorption coefficient or adsorption capacity,  $1/n$  is an empirical linearization constant or adsorption intensity. It fitted well for potassium adsorption onto kaolin clay. Figure 11 shows that the Freundlich adsorption coefficient ( $K_f$ ) increased

with increasing temperature. The potassium adsorption onto kaolin clay in this study can be explained by two possible adsorption mechanisms. Potassium is basically an exchangeable cation. The lower pH was observed at 40 °C because of temperature dependent autoionization (self-ionization) property of water ( $K_w$ ) which might reduce the pH of solution at high temperature. At low pH, kaolin edge surface possesses more positive charges since point of zero charge (PZC) for kaolinite ranges from 3.5 to 4 (Mon *et al.* 2012). Hence, cation exchange mechanism may occur by exchange  $K^+$  with the positive charge like  $H^+$  on the kaolin edge surface. Second possible adsorption mechanism was electrostatic ion exchange mechanism mainly at 6 °C because the observed pH was greater than 4 of PZC and then kaolin edge surface may possess more negative charges. Electrostatic ion exchange might occur by attraction of negative charge on clay surface to positive charge of potassium. Accordingly, cation exchange mechanism was supposed to be a dominant adsorption mechanism since the greater potassium adsorption onto kaolin clay was observed at 40°C as compared to at 6 °C.

Another approach based on equilibrium sorption described that the calculated retardation factor ( $R_d$ ) as a function of ion concentration was nonlinearly correlated (Fig 12). Sharma and Reddy (2004) proposed the following equation for the calculation of  $R_d$  using Freundlich adsorption coefficient and intensity ( $K_f$  and  $1/n$ ).

$$R_d = 1 + \left( \frac{\rho_d}{\theta_{sat}} K_f \frac{1}{n} C_e^{\left(\frac{1}{n}-1\right)} \right) \quad (7)$$

where  $R_d$  is retardation factor,  $\rho_d$  is dry bulk density ( $g/cm^3$ ) and  $\theta_{sat}$  is volumetric water content ( $cm^3/cm^3$ ). Here, the average dry bulk density and volumetric water content values for samples with high  $e_0$  from solute diffusion experiments was used

to calculate  $R_d$ . The relative concentration used in solute diffusion experiment was about 4000 ppm obtained from 0.1M KCl solution. It can be seen that the  $R_d$  was only about 1.2. This result was in agreement with the observation in diffusion tests. Because the solute diffusion coefficient ( $D_s$ ) for potassium was lower than  $D_s$  for chloride with  $D_s(\text{Cl})/D_{s,\text{app}}(\text{K})$  of the values from 1.1 to 1.2 meaning that only 10 to 20% of potassium was retarded as compared to chloride. Therefore, retardation factor was significantly affected by ion concentration. It can be suggested that potassium ion likely behaves as a conservation ion if the very high concentration of potassium is used in transport experiments.

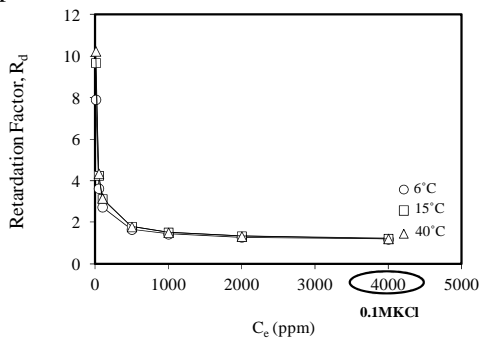


Figure 12 Effects of ion concentration on retardation factor.

In addition, both kinetic and thermodynamic results (i.e. the larger rate constant at higher temperature (40 °C), and the positive activation energy values) also implied that higher temperature enhanced the adsorption of potassium onto kaolin clay. Accordingly, it can be explained that the cation exchange mechanism at higher temperature (40 °C) resulted from temperature dependent pH property was probably a dominant adsorption mechanism for potassium adsorption onto kaolin clay.

## 4. CONCLUSIONS

### 4.1 Temperature effects on geotechnical properties of clay

The simultaneous measurements of consolidation characteristics, shear stiffness, and permeability of preconsolidated kaolin clay under sequential consolidation pressures were conducted at different temperatures (5 °C, 15 °C, and 40 °C) by using modified oedometer apparatuses. Temperature influence on consolidation parameters such as the apparent preconsolidation pressure ( $P_{ac}$ ) markedly increased with increasing temperature while compression index ( $C_c$ ) slightly increased for H 10 cm and H 2 cm samples with high  $e_0$  ( $1.5 < e_0 < 1.65$ ). The shear modulus ( $G_{b,e}$ ) as a function of void ratio resulted from the successive applied consolidation pressures at 40 °C was larger than that at 5 °C even at the same void ratio. The trend of the measured  $G_{b,e}$  as a function of void

ratio closely followed previous empirical formulas for predicting shear modulus. The increase in  $G_{b,e}$  at higher temperature was explained by inter-particle contacts enhanced by inter-particle forces between particles resulted from the decrease in dielectric constant property of pore water at 40 °C. Temperature effects on the permeability ( $k$ ) of kaolin clay as a function of void ratio were not significant within the studied temperature range between 5 °C and 40 °C. The pore size distribution measurements verified this observation by indicating similar pore structure of the tested samples at 5 °C and 40 °C, and then, giving similar permeability. Despite the similar permeability of clay as a function of void ratio within the studied temperature range, the saturated hydraulic conductivity ( $K_{sat}$ ) was basically affected by temperature due to temperature dependent pore water viscosity and water density properties.

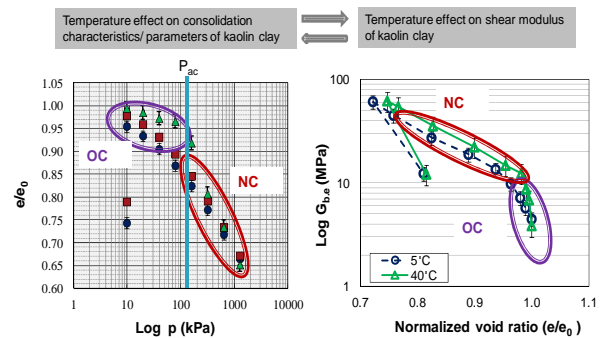


Figure 13 The inter link between consolidation and shear stiffness properties of the sample under consolidation.

As shown in Fig. 13, it can be considered that temperature effects on consolidation parameter ( $P_{ac}$ ) and shear stiffness ( $G_{b,e}$ ) property of a tested sample were interrelated each other. Because OC condition illustrated in  $e/e_0$  -  $\log p$  curve corresponded to that in  $G_{b,e}$  vs  $e/e_0$  relationship showing the variation with temperature. Similar slopes were obtained under different temperature for NC condition in both  $e/e_0$  -  $\log p$  curve and  $G_{b,e}$  vs  $e/e_0$  relationship. Consequently, the combined measurements of consolidation, shear stiffness and permeability and pore structure investigation provided a unified understanding that for sample with high  $e_0$  ( $1.5 < e_0 < 1.65$ ), the changes in fabric structure (likely caused by enhanced inter-particle forces between clay particles at higher temperature) would result in the increased shear stiffness and, consequently, higher  $P_{ac}$  at elevated temperature (40 °C).

The investigation was extended to certify the consolidation and shear stiffness properties induced by temperature elevation observed in part I. Thus, for preconsolidated kaolin samples with high  $e_0$  ( $1.5 < e_0 < 1.65$ ) and low  $e_0$  ( $1.4 < e_0 < 1.5$ ), change in

consolidation settlement and shear modulus was simultaneously measured under temperature elevation from 15 °C to 40 °C in the secondary compression stage at two consolidation pressures representing OC state and NC state. For both OC and NC clays, the decrease in normalized void ratio was observed after being heated for 7 days implying that heating reactivated the consolidation settlement in secondary compression stage. It was supported that the lower water viscosity at 40 °C accelerated the clay particle arrangements under a substantial stress. After temperature elevation for 7 days, the larger shear modulus ( $G_2$ ) was attained for OC samples with both void ratios while  $G_2$  did not recover back to the value of  $G_1$  for NC samples. For OC samples, the greater shear stiffness was probably contributed not only by the increase in consolidation settlement but also by the closer inter-particle arrangements caused by smaller dielectric constant at 40 °C. For NC sample, the behavior of change in shear modulus was quite similar to the results obtained for saturated sand samples indicating that this behavior resulted only from the temperature dependence of bender element performance and it is not representing the real shear stiffness response affected by temperature. In summary, it can be suggested that effect of temperature elevation was stress history dependent and consolidation and shear stiffness properties of the samples with high  $e_0$  under OC state were highly depended on temperature elevation. The observation in part I in which greater stiffness at 40 °C since at 9.8 kPa corresponded to OC state was found for H 10 samples with high  $e_0$  verified this assumption. Therefore, for the clays with high  $e_0$ , the increase in soil temperature can cause the consolidation settlement but with the greater shear stiffness of the clays.

#### 4.2 Temperature effects on solute transport processes in clay

Temperature effects on solute diffusion, one of the major solute transport processes, in preconsolidated kaolin clays were investigated through the tracer solution of potassium chloride (KCl) at different temperatures (6 °C, 15 °C, 40 °C) using specified volume diffusion (SVD) apparatuses. Both cation ( $K^+$ ) and anion ( $Cl^-$ ) diffusion behaviors as a function of temperature were examined for samples with high  $e_0$  (1.65) (at  $\rho=1.0 \text{ Mg m}^{-3}$ ) and low  $e_0$  (1.15) (at  $\rho=1.2 \text{ Mg m}^{-3}$ ). For both ions, the relative concentration in the source chamber decreased with time while  $C_s/C_0$  in the receptor chamber increased with time for both kaolin clays mainly due to the solute diffusion from the source to the receptor through the clay. The solute diffusion coefficients ( $D_s$  or  $D_{s,app}$ ) of both  $Cl^-$  and  $K^+$  were evaluated using two-chamber semi-analytical method. The precise  $D_s$  values

corresponding to change in concentration in the receptors were deduced by linearization of the measured data with extreme high coefficient of regression for all cases. The positive correlations between solute diffusion coefficient ( $D_{s,app}$ ) and temperature for both anion and cation diffusions in both types of samples were observed showing that  $D_s$  increased by around  $(0.031 \text{ to } 0.036) \times 10^{-10} \text{ m}^2 \text{ s}^{-1}$  times temperature for  $Cl^-$  and  $(0.027 \text{ to } 0.033) \times 10^{-10} \text{ m}^2 \text{ s}^{-1}$  times temperature for  $K^+$ . The  $D_s$  for  $Cl^-$  ion were relatively higher than the  $D_{s,app}$  for  $K^+$  ion with the ratio of  $D_s(Cl^-)/D_{s,app}(K^+)$  ranging only from 1.1 to 1.2 mostly due to the retardation of  $K^+$  ion on kaolin clay which was proofed by the observation of  $K^+$  adsorption onto kaolin clay in the next chapter. The solute diffusivity of  $K^+$  and  $Cl^-$  ions as a function of water-saturated porosity (correlated to void ratio) was tested against the literature data for solute diffusivity of inorganic chemicals in different types of soils as well as for gas diffusivity in different type of soils and clay minerals by applying existing linear Penman model and non-linear power models. Existing models were quite applicable mostly for solute diffusion and gas diffusion in natural soils. The greater solute diffusivity was exhibited at high  $e_0$  or lower bulk density: with  $D_s/D_0 \sim 1/6\theta_{sat}$  (water-saturated porosity) using linear model and with  $D_s/D_0 \sim (\theta_{sat})^{4.4}$  using non-linear power model. Thus,  $D_s/D_0$  for both ions in kaolin clay was basically lower than that in soils possibly due to the finer pores in kaolin clay reducing the solute diffusion efficiency through greater liquid phase tortuosity. Furthermore, clay pore system is seemed to be mostly inactive for solute diffusion particularly in bentonite. The observations in this part would partly be useful for not only risk assessments of ground water pollution but also design of land fill clay liner systems in waste disposal sites.

Temperature effects on potassium chloride (KCl) sorption on kaolin clay were investigated by performing batch adsorption experiments under different concentrations and at three temperatures (6 °C, 15 °C, 40 °C). There was almost no retardation of  $Cl^-$  while  $K^+$  adsorption onto the clay was observed at all temperatures. Generally, the sorption isotherms were fitted well with both Freundlich model. The higher adsorption coefficient ( $K_f$ ) was exhibited at higher temperature probably due to the enhanced cation exchange mechanism for exchangeable potassium adsorption onto kaolin clay at 40 °C. The value of retardation factor ( $R_d$ ) increased with increasing temperature and ion concentration. The potassium at very high concentration was rarely retarded onto kaolin clay. This result verified the observation in solute diffusion tests that diffusion of potassium was slightly lower than chloride with the ratio of only 1.1 to 1.2. Thus, it can be hypothesized that

potassium ion behaves likely as a conservation ion at very high concentration. Additionally, both kinetic and thermodynamic results (i.e. the larger rate constant at higher temperature (40 °C), and the positive activation energy values) also indicated that higher temperature enhanced the adsorption of potassium onto kaolin clay.

#### 4.3 Knowledge towards a unified understanding of temperature effects on geotechnical properties of clays and solute transport processes in clays

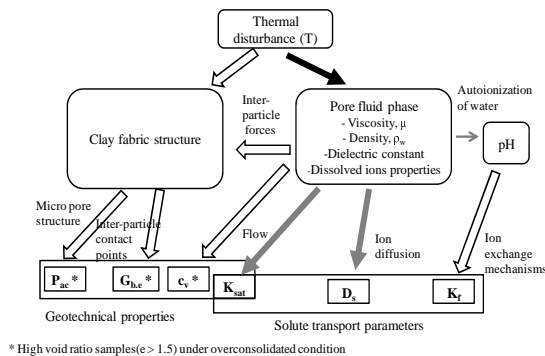


Figure 14 Representative diagram illustrated for a unified understanding of temperature (thermal disturbance) effects on both geotechnical properties of clay and solute transport processes in clay.

This research attributes to a basic knowledge towards a unified understanding of temperature effects on geotechnical properties and solute transport process in clay. Thermal disturbance in geo-environments (change in subsurface temperature) affects clay fabric structure and pore fluid phase (for example: pore fluid properties such as pore water viscosity and pore water density, dielectric constant properties, and dissolved ions properties such as ion motion which was driven by thermal motion). The dielectric constant property is inversely related to inter-particle forces between particles and it probably changes the clay fabric structure. Change in clay fabric structure causes change in geotechnical properties of  $P_{ac}$  and  $G_{b,e}$  through alteration in inter-particle contact points and micro pore structure. Variation of pore fluid properties directly influences the one of the geotechnical properties,  $c_v$ , and one of the transport properties saturated hydraulic conductivity ( $K_{sat}$ ) which is correlated to permeability of clay ( $k$ ). Pore fluid viscosity and dissolved ions driven by thermal variation generate the change in solute diffusion coefficients. Moreover, temperature dependent autoionization of water causes change in pH of solution resulting in adsorption efficiency variation. In accordance with the observation in the research, temperature effects on these three geotechnical properties ( $P_{ac}$ ,  $G_{b,e}$ , and  $c_v$ ) are highly pronounced for sample with high initial void ratio and

overconsolidated stage. The black arrow shows the major property directly affected by temperature. The gray arrows indicate medium tendency of temperature influence on  $K_{sat}$  and  $D_s$ . The white arrows show the properties indirectly affected by temperature. Further study should be done to clarify and strongly devote the temperature effects on those properties and the more other parameters or factors may include in this understanding.

#### 5. REFERENCES

- Abuel-Naga, H.M., Bergado, D.T., Ramana, G.V., Rujivipat, P., and Thet, Y., (2006) "Experimental evaluation of engineering behavior of soft Bangkok clay under elevated temperature," *J. Geotech. Geoenviron. Eng.*, ASCE, **Vol. 132**, (No. 7), pp. 902-910.
- Anderson D.G. and Stokoe K.H., (1978) "Shear modulus: A time dependent soil property," *Dynamic Geotechnical Testing, ASTM STP 654*, American Society for Testing and Materials, pp 66-90.
- Bonte, M., Stuyfzand, P.J., Hulsmann, A., and Beelen, P.V., (2011). "Underground thermal energy storage: Environmental risks and policy developments in the Netherlands and European Union," *Ecol. and Soc.*, **Vol. 16**, (No. 1), 22. [online]
- Boudali, M., Leroueil, S., and Srinivasa Murthy, B.R., (1994) "Viscous behaviour of natural clays." *Proceedings 13<sup>th</sup> International Conference on Soil Mechanics and Foundation Engineering*, New Delhi, **Vol. 1**, pp. 411-416.
- Buckingham, E., (1904). "Contributions to our knowledge of the aeration of soils," *USDA. Bur. Soil Bull. 25*. U.S. Gov. Print. Office, Washington, DC.
- Campanella, R. G. and Mitchell, J. K., (1968) "Influence of temperature on soil behavior." *J. Soil Mech. Found. Eng. Div.*, ASCE, **Vol. 94**, (No. 3), pp. 709-734.
- Chan, C.-M., (2010) "Bender element test in soil specimens: Identifying the shear wave arrival time," *Electron. J. of Geotech. Eng.*, **Vol. 15**, pp. 1263-1276.
- Crawford, C.B., (1964) "Interpretation of the consolidation test," *J. Soil Mech. Found. Div.*, ASCE, **Vol. 90**, pp. 87-102.
- Do, N. Y., and Lee, S. R., (2006) "Temperature effect on migration of Zn and Cd through natural clay," *Environ. Monit. and Assess.*, **Vol. 118**, pp. 267-291.
- Florides, G., Kalogirou, S., (2007) "Ground heat exchangers-a review of systems, models and

applications,” *Renewable Energy*, **Vol. 32**, pp. 2461-2478.

Habibagahi, K., (1973) “Temperature effect on consolidation behaviour of overconsolidated soils,” *8<sup>th</sup> Int. Conf. Soil Mechanics and Foundation Engineering*. Moscow, **Vol. 1**, pp. 159-162.

Haehnlein, S., Bayer, P., and Blump, P., (2010) “International legal status of the use of shallow geothermal energy,” *Renew. Sustain. Energy Rev.* **Vol. 14**, pp. 2611-2625.

Lambe, T.W., (1960) “Compacted Clay,” *Trans. Am. Soc. Civ. Eng.*, 125 (Part I), pp. 682-756.

Lee, J.-S., and Santamarina, J.C., (2005) “Bender elements: Performance and signal interpretation,” *J. Geotech. Geoenviron. Eng.*, ASCE, **Vol. 131**, (No. 9), pp. 1063-1070.

Marshall, T. J., (1959) “The diffusion of gases through porous media,” *J. Soil Sci.*, **Vol. 10**, pp. 79-82.

Millington, R. J., (1959) “Gas diffusion in porous media,” *Science* (Washington, DC) 130, pp. 100-102.

Mon, E. E., Sharma A., Hamamoto, S., Kawamoto, K., Hiradate, S., Komatsu, T., and Moldrup, P., (2012) “The pH dependency of 2,4-dichlorophenoxyacetic acid adsorption and desorption in Andosol and kaolinite,” *Soil Science*, **Vol. 177**, (No. 1), 12-21.

Nakagawa, K., Soga, K., Mitchell, J.K., and Sadek, S., (1995) “Soil structure changes during and after consolidation as indicated by shear wave velocity and electrical conductivity measurements.” *Proceedings, Compression and consolidation of clayey soils*, IS-Hiroshima, Balkema, Rotterdam, **Vol. 2**, pp. 1069-1074.

Omer A.M., (2008) “Ground-source heat pumps systems and applications,” *Renew. Sust. Energ. Rev.*, **Vo. 12**, pp. 344-371.

Penman, H. L., (1940) “Gas and vapor movements in soil: The diffusion of vapors through porous solids,” *J. Agric. Sci.*, **Vol. 30**, pp. 437-462.

Rao, S.M., and Sridharan, A., (1985) “Mechanism controlling the volume change behavior of kaolinite,” *Clay. Clay Miner.*, **Vol. 33**, (No. 4), pp. 323-328.

Rowe, R. K., Lake C. B., and Petrov, R. J., (2000) “Apparatus and procedures for assessing inorganic diffusion coefficients for geosynthetic clay liners.” *Geotechnical Testing Journal, GTJODJ*, **Vol. 23**, (No. 2), pp. 206-214.

Rowe, R. K., Mukunoki T., and Sangam H. P., (2005) “BTEX diffusion and sorption for a geosynthetic clay liner at two temperatures,” *Journal of Geotechnical and Geoenvironmental*

*Engineering. ASCE.* **Vol. 131**, (No. 10), pp. 1211-1221.

Schediegger, A. E. (1957). *The physics of flow through porous media*, The Macmillan Company, New York.

Sharma, H. D. and Reddy, K. R., (2004) “Geoenvironmental Engineering, Site Remediation, Waste Containment, and Emerging Waste Management Technologies,” John Wiley & Sons, Inc., Hoboken, New Jersey, Chapter 8.

Shimizu, M., (2003) “Quantitative assessment of thermal acceleration of time effects in one-dimensional compression of clays” *Proc. 3rd Int. Symp. On Deformation Characteristics of Geomaterials*, Lyon, pp. 479-487.

Sowers, L., York, K., and Stiles, L., (2006) “Impact of thermal buildup on groundwater chemistry and aquifer microbes.” *10<sup>th</sup> International Conference on Thermal Storage-Ecostock: Thermal Energy Storage Here and Now*, Stockton, USA.

Spitler, J.D., (2005) “Ground-source heat pump system research-past, present, and future,” *HVAC&R Research*, **Vol. 11**, pp. 165-167.

Sridharan, A., and Rao, G.V., (1979) “Shear strength behaviour of saturated clays and the role of the effective stress concept,” *Geotechnique.*, **Vol. 29**, (No. 2), pp. 177-193.

Sultan, N., Delage, P., and Cui, Y.J., (2002) “Temperature effects on the volume change behavior of Boom clay,” *Eng. Geol.*, **Vol. 64**, pp. 135-145.

Taniguchi, M., Uemura, T., and Jagon-on, K., (2007) “Combined effects of urbanization and global warming subsurface temperature in four Asian cities,” *Vadose Zone J.*, Vol. 6, pp. 591-596.

Tidfors, M., and Sällfors, G., (1989) “Temperature effect on preconsolidation pressure.” *Geotechnical Testing Journal.*, **Vol. 12**, (No. 1), pp. 93-97.

Towhata I., Kuntiwattanaku P., Seko I., and Ohishi K., (1993) “Volume change of clays induced by heating as observed in consolidation tests,” *Soils Found., Japanese Society of Soil Mechanics and Foundation Engineering*, **Vol. 33**, (No. 4), pp. 170-183.

Virdi, S.P.S., and Keedwell, M.J., (1988) “Some observed effects of temperature variation on soil behavior,” In: m.J. Keedwell (Editor), *Int. Conf. Rheology and Soil Mechanics*, Coventry, Sept. 1988. Elsevier Applied Science Publishers, London, pp. 336-354.